Carbohydrate Polymers 94 (2013) 449–455

Contents lists available at SciVerse ScienceDirect

Carbohydrate Polymers

journal homepage: www.elsevier.com/locate/carbpol

pH-responsive sodium alginate-based superporous hydrogel generated by an anionic surfactant micelle templating

Xiaoning Shi[a,b], Wenbo Wang[a,c], Aiqin Wang[a,c,*]

[a] R&D Center of Xuyi Attapulgite Applied Technology, Lanzhou Institute of Chemical Physics, Chinese Academy of Sciences, Lanzhou 730000, China
[b] Gansu University of Traditional Chinese Medicine, Lanzhou 730000, China
[c] Key Laboratory of Chemistry of Northwestern Plant Resources, Chinese Academy of Sciences, Lanzhou 730000, China

ARTICLE INFO

Article history:
Received 20 August 2012
Received in revised form 6 November 2012
Accepted 14 January 2013
Available online 21 January 2013

Keywords:
Superporous hydrogel
SDS micelle templating
Sodium alginate
Morphology
Swelling kinetics

ABSTRACT

A novel sodium alginate-based superporous hydrogel (SPH) was prepared by the grafting copolymerization and micelle templating formed by the self-assembled anionic surfactant sodium *n*-dodecyl sulfonate (SDS). Fourier transform infrared (FTIR) spectra demonstrated that SDS was removed from the final hydrogel network. The formation mechanism of NaAlg-based SPH was proposed. Effect of SDS concentration on the morphologies and pore structure of the hydrogel was evaluated by Scanning Electron Microscopy (SEM), and the SDS-1.92 mM sample displays homogeneous and well-defined pores, which contribute to improve swelling ratio and swelling rate. The time-dependent swelling behaviors of the SDS-1.92 mM samples in various salt and pH solutions were investigated. The swelling in multivalent salt (Ca^{2+}, Al^{3+})/pH 2 solutions displayed a well-known "overshooting effect", whereas, its swelling kinetics in Na^{+}/pH 3–12 solutions followed Schott's pseudo second-order swelling kinetics model.

1. Introduction

Hydrogels are lightly cross-linked polymeric network that are capable of swelling and absorbing large amounts of water without losing their physical dimension structure. Applications of hydrogels range from traditional agriculture to pharmaceutics (Almeida, Ferreira, Lopes, & Gil, 2011; Foungfung, Phattanarudee, Seetapan, & Kiatkamjornwong, 2011; Ozay, Ekici, Baran, Aktas, & Sahiner, 2009; Van Vlierberghe, Dubruel, & Schacht, 2011; Zohuriaan-Mehr, Omidian, Doroudiani, & Kabiri, 2010). Among them, superporous hydrogels (SPHs) are of particular interest and show great potential in various pharmaceutical and biomedical applications (Gils, Ray, & Sahoo, 2009; Jia, Young, & Moo, 2011; Yin et al., 2010). The advantageous fast swelling of SPHs is for a consequence of their interconnected open cellular structure. The superporous structure allows the faster diffusion of water molecules into the polymer network by reducing the transport resistance, and endows the hydrogels with additional space to hold more water. So, SPHs can generate rapid response to the external stimuli and possess higher total swelling capacity.

The creation of porosity in the hydrogels is the key to regulating the properties. Currently, available techniques for fabricating a porous hydrogel mainly include freeze-drying (Poursamara, Azamib, & Mozafari, 2011), gas-foaming (Park & Kim, 2006), water-soluble porogens (Delaney, Liberski, Perelaer, & Schubert, 2010) and phase-separation (Elbert, 2011). Among all of these techniques, the contradiction between the control of porosity and the convenience for pore-forming operation becomes a limiting factor. Emulsion templating is a facile approach for producing a well-defined and controllable pore structure (Busby, Cameron, & Jahoda, 2001; Cameron, 2005; Partap, Muthutantri, Rehman, Davis, & Darr, 2007; Partap, Rehman, Jones, & Darr, 2006). In aqueous solution, surfactants can self-assemble with each other to form micelles. These micelles can act as a template in the polymerization reaction to form porous materials with controlled pore size and applied in drug delivery system (Lee et al., 2010), tissue engineering (Barbetta, Barigelli, & Dentini, 2009; Ji, Khademhosseini, & Dehghani, 2011) and waste-water treatment (Chatterjee, Chatterjee, & Woo, 2010; Chatterjee, Lee, Lee, & Woo, 2010).

Recently, with the excessive consumption of petroleum resources and the increase in environmental pollution, natural polysaccharides have received great concerns as a renewable, biodegradable, non-toxic and biocompatible "green material". Thus many polysaccharides including starch (Pang, Chin, Tay, & Tchong, 2011), cellulose (Chang, Duan, Cai, & Zhang, 2010), chitosan (Zhou, Ma, Shi, Yang, & Nie, 2011), alginate (Yang, Ma, & Guo, 2011) as well as the protein gelatin (Pourjavadi, Hosseinzadeh, & Sadeghi,

* Corresponding author at: R&D Center of Xuyi Attapulgite Applied Technology, Lanzhou Institute of Chemical Physics, Chinese Academy of Sciences, Lanzhou 730000, China. Tel.: +86 931 4968118; fax: +86 931 827708.
E-mail addresses: aqwang@licp.cas.cn, aqwang@lzb.ac.cn (A. Wang).

0144-8617/$ – see front matter © 2013 Elsevier Ltd. All rights reserved.
http://dx.doi.org/10.1016/j.carbpol.2013.01.019

2007) were utilized as starting materials for fabricating superabsorbent hydrogels. Sodium alginate (NaAlg) is a naturally occurred colloidal hydrophilic polysaccharide extracted from the brown seaweed (phaceophyceae) (Draget, SkjakBraek, & Smidsrod, 1997). It is a linear block copolymer consisting of (1,4)-α-L-glucuronic acid (G units) and (1,4)-β-D-mannuronic acid (M units), and was extensively used in foods, pharmaceuticals and agricultural areas (Augst, Kong, & Mooney, 2006). NaAlg with higher carboxylic content is expected to have superior hydrophilic properties and potential in absorbent applications. Many reports were available on the synthesis of superabsorbent hydrogels from NaAlg and multifunctional vinyl monomers (Cha, Kim, Kim, & Kong, 2011; Dumitriu, Mitchell, & Vasile, 2011; Sand, Yadav, Mishra, & Behari, 2010), but no substantial research on NaAlg-based SPHs preparing by micelle templating technique has been reported.

Based on our previous work for polysaccharides-based superabsorbent hydrogels (Shi, Wang, & Wang, 2011a; Shi, Wang, & Wang, 2011b), we prepared sodium alginate-*g*-poly(sodium acrylate-*co*-styrene)/attapulgite (NaAlg-*g*-P(NaA-*co*-St)/APT SPH using an anionic surfactant sodium *n*-dodecyl sulfonate (SDS) as the pore-forming templating. Fourier transform infrared (FTIR) spectra were used to confirm the successful synthesis of NaAlg-*g*-P(NaA-*co*-St)/APT hydrogel and removal of SDS from the final products by washing process. The effect of SDS concentration on the porosity of the hydrogel was investigated by Scanning Electron Microscopy (SEM). In addition, the effect of swelling medium (e.g. ionic strength and charge, pH) on the swelling kinetics of this SPH was investigated and analyzed by Schott's pseudo second-order swelling kinetics model.

2. Materials and methods

2.1. Materials

Sodium alginate (NaAlg) was purchased from Shanghai Chemical Reagents Corp. (Shanghai, China). Attapulgite clay (APT, milled and passed through a 200-mesh screen prior to use) was supplied by Gaojiawa Colloidal Co. (Jiangsu, China). Acrylic acid (AA, CP) and styrene (St, CP) were purchased from Shanghai Wulian Chemical Factory (Shanghai, China). Ammonium persulfate (APS, AR) was purchased from Xi'an Chemical Reagent Factory (Xi'an, China). *N,N′*-methylene-*bis*-acrylamide (MBA, AR) was purchased from Shanghai Chemical Reagent Corp. (Shanghai, China). Sodium *n*-dodecyl sulfonate (SDS) was also obtained from Shanghai Chemical Reagent Corp. (Shanghai, China) and used as received. Other agents used were all analytical grade, and all solutions were prepared with distilled water.

2.2. Preparation of NaAlg-g-P(NaA-co-St)/APT SPHs

NaAlg (1.20 g) was dissolved in 20 mL distilled water in a 250 mL four-necked flask under stirred at 60 °C. Then, a certain amount of SDS aqueous solution (0, 0.96, 1.92, 2.88 and 3.84 mM) was added and the mixture was stirred for 30 min to form a homogenous solution. The solution was purged with nitrogen to remove the dissolved oxygen, and 5 mL aqueous solution of initiator APS (0.100 g) was introduced and kept at 60 °C for 15 min to generate radicals. Afterward, the reaction system was cooled to 40 °C, and the mixture solution containing AA (7.20 g, 70% neutralized degree), St (0.150 g), crosslinker MBA (0.0216 g) and APT (0.928 g) was added. The reaction temperature was increased to 70 °C and maintained for 3 h to complete the polymerization reaction. The hydrogel product was firstly washed with ethanol/water (*v*/*v*, 7:3) to remove SDS, and then dehydrated by absolute ethanol. The dried product was ground and passed through 40–80 meshes (the particle size is 180–380 μm).

2.3. Measurement of swelling ratio

A conventional gravimetric method was adopted to determine the swelling ratio of the SPHs. Typically, 0.050 g of dry sample was immersed in 200 mL swelling medium at room temperature for 2 h to reach swelling equilibrium. The swollen hydrogel was filtrated from the unabsorbed water by a 100-mesh sieve, and drained for 10 min until no droplet drip down. The swelling ratio (S_{eq}, g/g) of the superporous hydrogel was calculated according to Eq. (1).

$$S_{eq} = \frac{m_s - m_d}{m_s} \quad (1)$$

Here, m_d is the mass of dried sample (g), and m_s is the mass of swollen hydrogel (g). The data points represent mean ± SD from three repeated experiments.

2.4. Measurement of swelling kinetics

0.050 g dry sample was soaked in 200 mL swelling medium. At certain time intervals, the swelling ratio at *t* (s) moment (S_t, g/g) was calculated according to Eq. (1), correlating the mass of the swollen hydrogel (m_t) at given time to the dry sample (m_d).

2.5. Characterizations

Fourier transform infrared spectroscopy (FTIR) of the dry samples was taken on a Nicolet NEXUS FTIR spectrometer in the wave-number region of 4000–400 cm^{-1} using KBr pellet. For investigating the effect of SDS concentration on the porosity of the hydrogels, the surface morphologies of the xerogels were recorded by an S-4800 Scanning Electron Microscopy (SEM) after sputter-coating the specimens with gold film.

3. Results and discussion

3.1. Preparation and characterization of NaAlg-g-P(NaA-co-St)/APT SPHs

A proposed mechanism for the formation of NaAlg-*g*-P(NaA-*co*-St)/APT SPHs by an anionic surfactant SDS micelle templating is shown in Scheme 1. In NaAlg solution, the self-assembly of SDS can form spherical micelles. In the process of grafting copolymerization and crosslinking, these micelles may be enclosed in the network and act as a template for pore-forming. After removed SDS micelles by a washing process, the superporous structure was generated.

FTIR spectroscopy was employed to verify the chemical structure of NaAlg-*g*-P(NaA-*co*-St)/APT hydrogel and removal of SDS

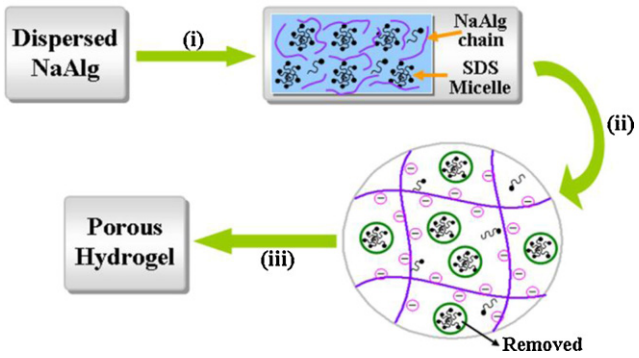

Scheme 1. Proposed reaction scheme for the synthesis of NaAlg-based SPHs using SDS micelle templating.

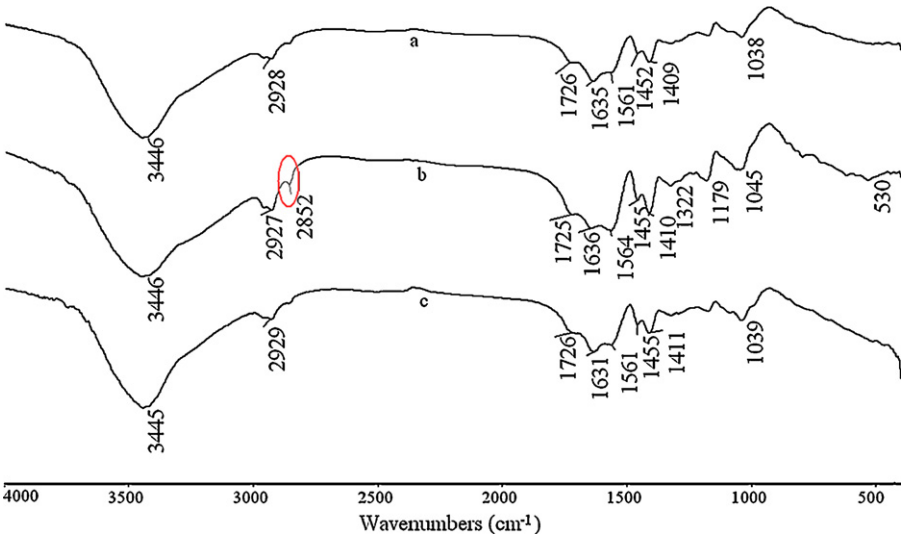

Fig. 1. FTIR spectra of (a) SDS-free hydrogel, (b) non-washed-SDS hydrogel and (c) washed-SDS hydrogel.

micelles from the polymeric network. As shown in Fig. 1, the broad absorption peaks at 3445–3446 cm^{-1} and 2927–2929 cm^{-1} can be ascribed to the O—H and C—H stretching vibration, respectively. The peaks at 1725–1726 cm^{-1} (C═O stretching vibration), at 1631–1635 cm^{-1} (asymmetric stretching vibration of the —COO^- groups), at 1561 cm^{-1} and 1455–1410 cm^{-1} (symmetric stretching vibration of the —COO^- groups) were observed (Shi, Wang, Kang, & Wang, 2012). The characteristic absorption of phenyl groups of St in this region was overlapped by the absorption of —COO^- groups. By comparing the FTIR spectra of non-washed-SDS hydrogel (Fig. 2b) and washed-SDS hydrogel (Fig. 2c), the typical peak appearing around 2850 cm^{-1} (the C—H stretching vibration of —CH_2— of the SDS molecule) were obviously weakened after the washing process (Wang & Wang, 2010). The O═S═O symmetrical and asymmetrical stretching bands of the sulfonate groups of SDS molecule were appeared at 1179 and 1322 cm^{-1} (Kabiri, Lashani, Zohuriaan-Mehr, & Kheirabadi, 2011), which disappeared in the spectrum of washed-SDS hydrogel. In addition, the profiles of the characteristic

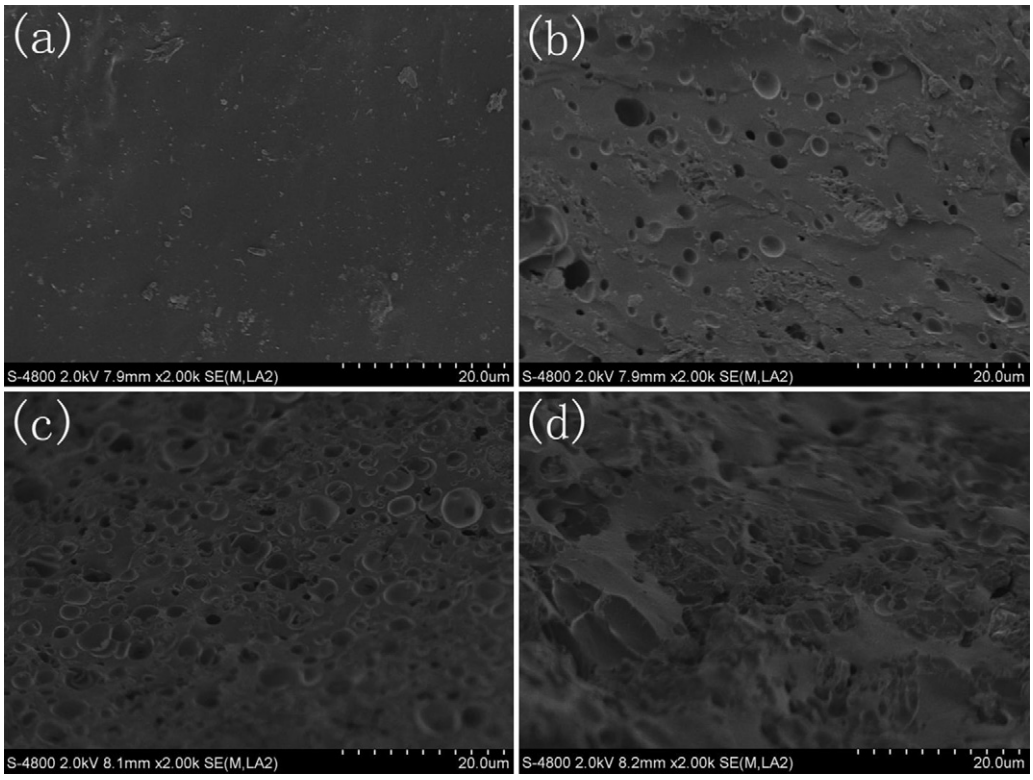

Fig. 2. SEM micrographs of (a) SDS-0 mM, (b) SDS-0.92 mM, (c) SDS-1.92 mM and (d) SDS-3.84 mM.

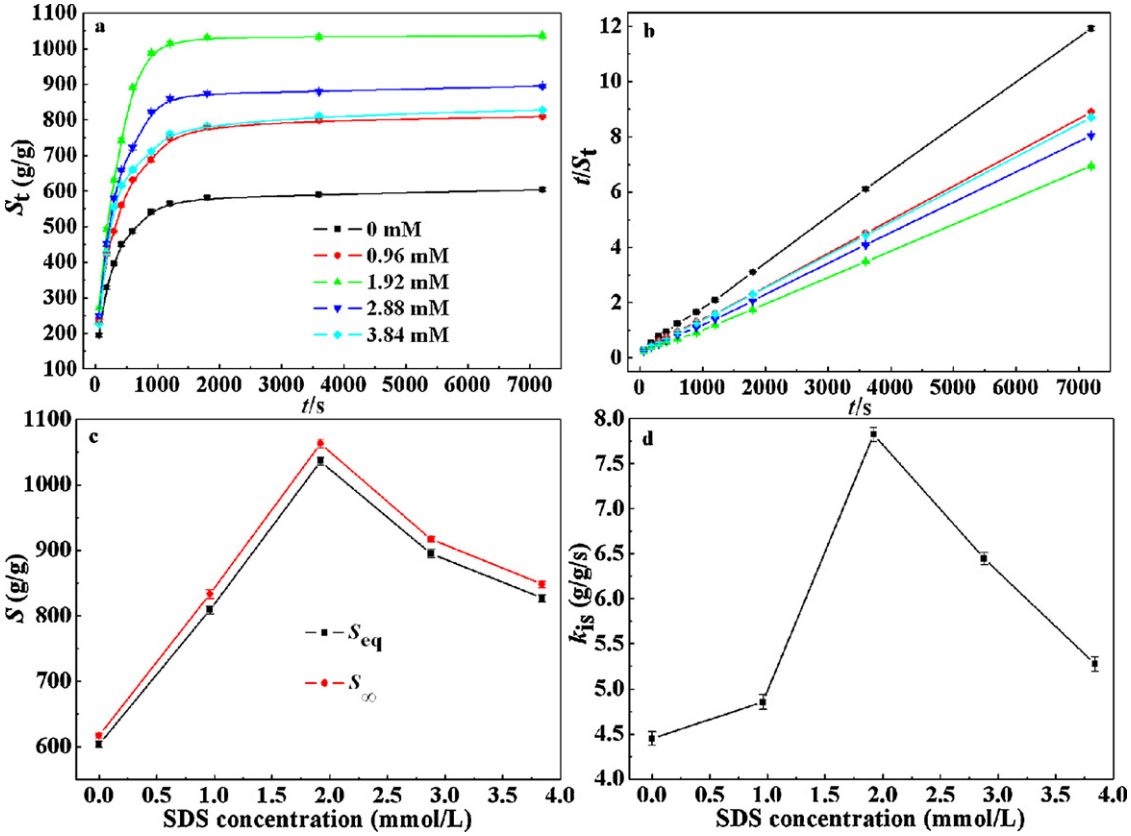

Fig. 3. (a) Time-dependent swelling curves of the SPHs generated by different concentration of SDS in distilled water, (b) their t versus t/S_t graphs according to Eq. (2), (c) their theoretical equilibrium swelling ratio (S_∞) and (d) initial swelling rate constant (k_{is}) data.

absorption peaks for SDS-free and washed-SDS hydrogel are almost identical, implying that all residual SDS have been removed from the hydrogel network (Fig. 2a and c).

3.2. Effect of SDS concentration on the morphologies and BET specific surface area

The effect of SDS concentration on the microstructure of NaAlg-*g*-P(NaA-*co*-St)/APT hydrogel was evaluated by SEM and BET analyses. As shown in Fig. 2a, the SEM micrograph of SDS-free sample presents a compact and non-porous surface, but SDS-added samples exhibit macroporous surface morphologies, and a gradual change in the pore density from Fig. 2b–d was observed. On the surface of SDS-0.96 mM sample, the pores were scattered. SDS-1.92 mM sample developed a continuous skin enveloped the skeleton of a macroporous interior. Thickness of the skin decreased with increasing SDS concentration and, hence, the impression of a porous skeleton was gradually reduced in SDS-3.84 mM sample (Fig. 2d). The gradual change in surface morphologies may be explained as follows. The pore structure of the hydrogel is mainly due to the self-assembling of SDS molecules in aqueous environment and the non-spherical micelles act as pore-forming templating (Partap et al., 2007). At lower SDS concentration (<1.92 mM), SDS mostly existed as dissociative ions and fails to generate enough micelles. Therefore, the presence of SDS did not significantly affect the network structure of the hydrogel. With increasing SDS concentration, micelles can be formed more easily, and act as a pore templating in the gelling process to produce a porous structure. With further increasing the SDS concentration, the porous skeletons of the hydrogel were more fragile and easy to collapse (Fig. 2d). In addition, the higher concentration of SDS possibly interfered with the gelling mechanism, which restricts the formation of the three-dimensional network of the hydrogel in the present reaction temperature (70 °C) (Su, Liu, Joshi, & Lam, 2008).

Table 1 listed the BET specific surface area and average pore size of the xerogels prepared with different SDS concentration. Compared with SDS-0 mM sample, the surface area and average pore size generated by SDS micelle templating were all enhanced, and SDS-1.92 mM sample shows the maximum surface area. The increased surface area and average pore size were favorable for improving the swelling ratio and swelling rate of the hydrogel.

3.3. Effect of SDS concentration on the swelling ratio and swelling kinetics

It has been demonstrated that the surface porosity of the hydrogel has greater influence on its swelling behaviors (Marsano, Bianchi, & Sciutto, 2003). As described above, the pore structure of NaAlg-*g*-P(NaA-*co*-St)/APT hydrogel is determined by SDS concentration. Fig. 3a plotted the variation of swelling ratio of the hydrogels with various concentrations of SDS as a function of swelling time. It is clear that the increase of swelling ratio was kinetically characterized by two parts: (i) the initial fast step and

Table 1
The BET specific surface area and the average pores size of the SPHs generated by SDS micelle templating.

Sample	BET specific surface area (m^2/g)	Average pore width (4 V/A by BET) (nm)
SDS-0 mM	0.7682	0
SDS-0.96 mM	2.7425	5.1756
SDS-1.92 mM	5.1756	11.0117
SDS-2.88 mM	3.6669	13.6572
SDS-3.84 mM	3.3872	9.2401

(ii) the asymptotical process to the equilibrium swelling ratio (S_{eq}). The S_{eq} value varied with altering the SDS concentration, and SDS-1.92 mM sample shows an optimal swelling ratio. As depicted above, SDS-1.92 mM sample had a more homogeneous pore structure and well-defined polymer network than the others, and the superporous structure facilitate the water molecules to enter the gel network more easily. The effect of SDS concentration on the swelling process was analyzed by a Schott's pseudo second-order swelling kinetics model (Schott, 1992):

$$\frac{t}{St} = \frac{1}{k_{is}} + \frac{1}{S\infty}t \quad (2)$$

where S_t is the swelling ratio at time t, S_∞ is the theoretical equilibrium swelling ratio, and k_{is} is the initial swelling rate constant. According to the experimental results shown in Fig. 3a, the plots of the average swelling rate (t/S_t) versus swelling time (t) give straight lines (Fig. 3b, $R^2 > 0.999$), indicating that the swelling process follows pseudo second-order swelling kinetic model. Fig. 3c and d illustrated the S_∞ and k_{is} values calculated from the slopes and intercepts of fitted straight lines. It was shown that theoretical S_∞ exhibits the same change tendency with S_{eq} when changing the SDS concentration (Fig. 3c). In addition, the initial swelling rate constant k_{is} also increased with increasing SDS concentration from 0 to 1.92 mM, but decreased with its further increase (Fig. 3d). It was known that the swelling of gel is a solvent diffusion and relaxation process of polymer chains (Rosa, Bordado, & Casquilho, 2002). The porosity of the gel contributes to enlarge specific surface area to speed up the diffusion rate of water molecules and improve the initial swelling rate. The k_{is} values for the hydrogels with different SDS concentration further confirmed that SDS-1.92 mM hydrogel has more and regular pores that facilitate to enhance the swelling rate.

3.4. Effect of salt solution on the swelling behaviors

The swelling behavior of the hydrogels is sensitive to salt concentration and ionic valences. Fig. 4a shows the time-dependent swelling behavior of SDS-1.92 mM sample in various concentrations of NaCl solutions, and the plots of t/S_t against t gives the straight line with the regression coefficient (R^2) higher than 0.999. As denoted in Eq. (2), the parameters k_{is} and k_s ($= k_{is}/S_\infty^2$) are the indication of swelling rate. It can be seen from Fig. 4b that the values of k_{is} rapidly decreased from 3.3874 to 1.3998 with increasing NaCl concentration from 0.1 mM to 15 mM. However, the values of k_s show a reverse tendency due to the alteration of swelling ratio (Eq. (2)). The initial swelling rate is related to a diffusion rate of water molecules, which was affected by the osmotic pressure difference between gel network and swelling medium (Zhao, Su, Fang, & Tan, 2005). Thus, the diffusion rate of water into the polymeric network (initial swelling rate) was reduced owing to the decrease in Donnan osmotic pressure with increasing NaCl concentration. Also, the increase of salt concentration results in the diminishing of electrostatic repulsion between polymer chains due to the screening of $-COO^-$ by Na^+, which limited the relaxation of the chains. The limited relaxation of the hydrogel means that the polymer chains need lesser time to reach the swelling equilibrium states, and thus the time to reach swelling equilibrium was greatly shortened and the swelling rate constant, k_s, is increased.

Fig. 5 depicted the time-dependent swelling characteristics of the hydrogel in 0.15 M NaCl, $CaCl_2$ and $AlCl_3$ solutions. It is obvious that the swelling kinetic curves in $CaCl_2$ and $AlCl_3$ solutions are different from that in NaCl solution. The swelling in $CaCl_2$ and $AlCl_3$ solutions shows the distinct "overshooting effect" swelling–deswelling phenomenon with prolonging the swelling time (Krušić & Filipovic, 2006). When the hydrogel was immersed in multivalent saline solution, the penetration of water molecules into the polymer network void leads to the expansion of hydrogel network. As a result, the expanded hydrogel network accelerates the diffusion of metal ions into the gel network, and then complexes with the hydrophilic $-COO^-$ groups. The ionic complexing interaction increased the crosslinking point in the interior or surface of hydrogel network, and caused the shrinkage of the swollen hydrogel. When the expansion of the hydrogel network and the contraction of network caused by ionic complexing action are

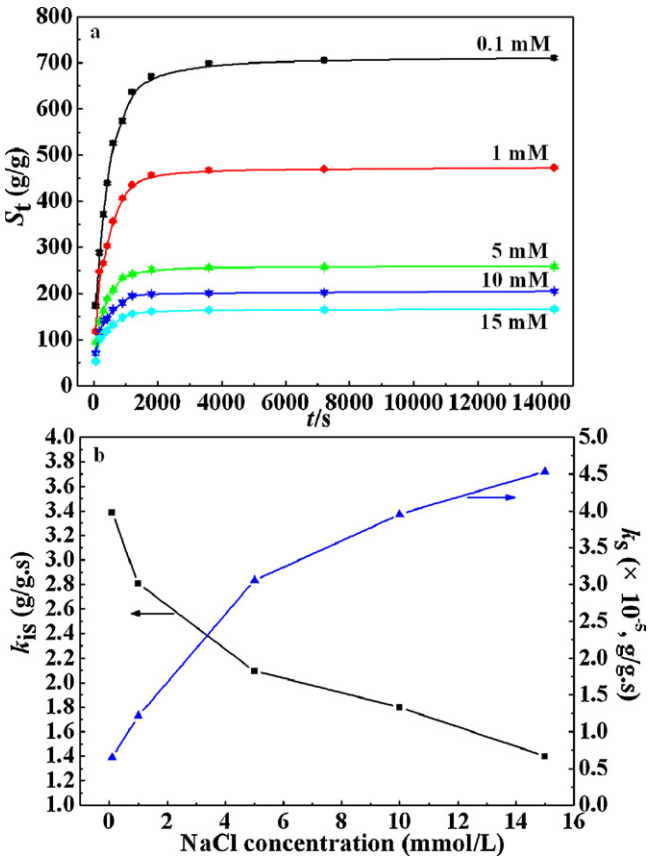

Fig. 4. (a) Time-dependent swelling curves of the SDS-1.92 mM sample in various NaCl solutions, (b) their initial swelling rate constant (k_{is}) and swelling rate constant (k_s) data, calculated according to Eq. (2).

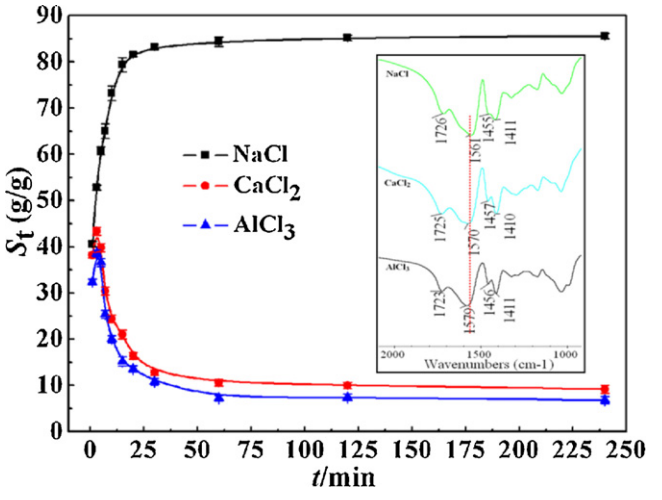

Fig. 5. The compared time-dependent swelling behaviors in 0.15 M NaCl, $CaCl_2$ and $AlCl_3$ solutions for SDS-1.92 mM sample and their FTIR spectra after swollen (inserted part).

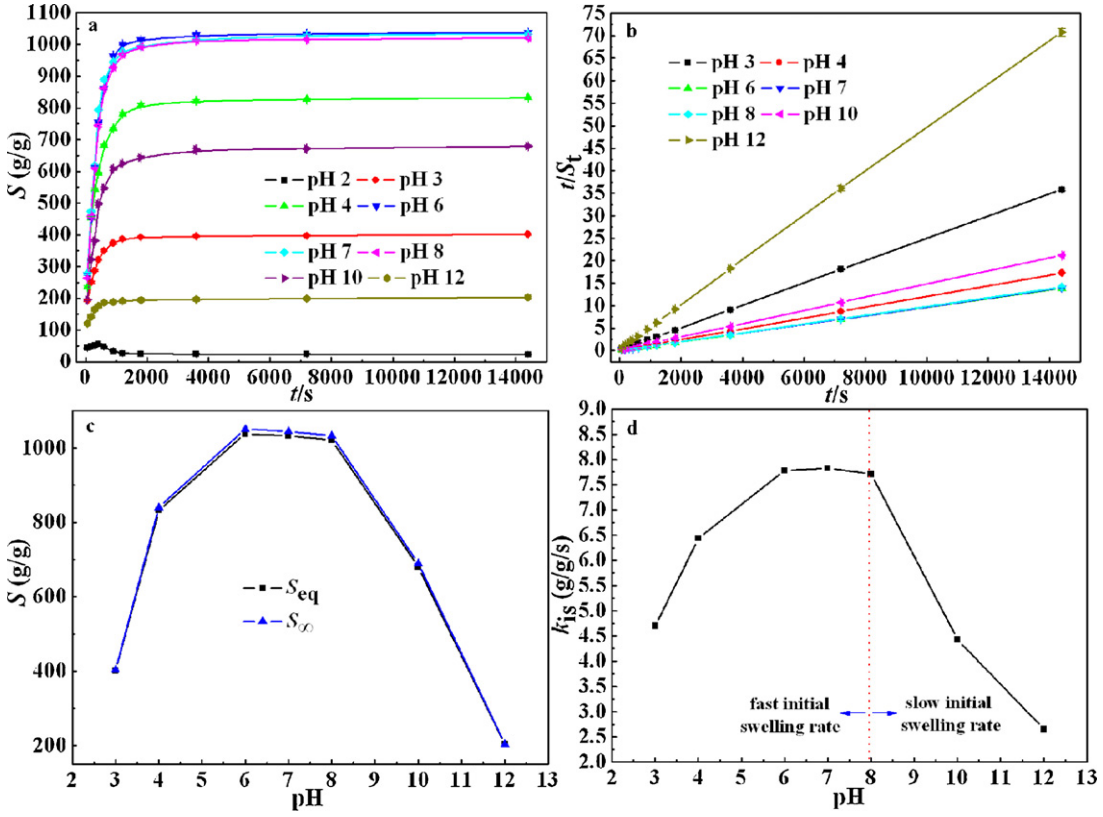

Fig. 6. (a) Time-dependent swelling curves of the SDS-1.92 mM sample in pH 2–12 solutions, (b) their t versus t/S_t graphs according to Eq. (2), (c) their theoretical equilibrium swelling ratio (S_∞) and (d) initial swelling rate constant (k_{is}) data.

equal, the hydrogel reached an equilibrium state. The changes of chemical environment of —COO^- groups of the SDS-1.92 mM superporous hydrogel after swelling in 0.15 M NaCl, $CaCl_2$ and $AlCl_3$ solutions were indicated by FTIR spectra (inserted in Fig. 5). The absorption band of —COO^- groups at 1561 cm^{-1} (Fig. 1a) did not change after swelling in NaCl solution, but shifted to 1570 cm^{-1} and 1579 cm^{-1} after swelling in $CaCl_2$ and $AlCl_3$ solutions, respectively. This result indicated the generation of complexation interaction between Ca^{2+}/Al^{3+} and —COO^- groups.

3.5. Effect of external pH on the swelling behaviors

The time-dependent swelling behaviors of the SDS-1.92 mM hydrogel were investigated by a sequential pH variation (Fig. 6a). The pH values of the solutions were adjusted by diluting HCl (pH 1.0) or NaOH (pH 13.0) solutions for avoiding the influence of ionic strength. As can be seen, the swelling kinetics of the SPH is dependent on the pH values of the swelling medium. The dynamic swelling behavior in pH 2 solution exhibited a well-known "overshooting effect" (Krušić & Filipovic, 2006), which was mainly caused by the gradual protonization of —COO^- functional groups and the cooperative physical cross-linking action resulting from the hydrogen-bonding among the neighboring —COOH groups. The time-dependent swelling behavior observed in pH 3–12 solutions is similar to that in distilled water and NaCl solution. For obtaining the swelling kinetic parameters (k_{is} and S_∞) in various pH solutions, the Schott's second-order kinetics model (Eq. (2)) was adopted and the plots of t/S_t versus t in pH 3–12 solutions ($R^2 > 0.999$) were shown in Fig. 6b. It was concluded that the swelling process of the hydrogel in pH 2 solution does not follow the second-order swelling kinetics.

The S_{eq} and S_∞ values in pH 3–12 solutions are depicted in Fig. 6c. It was found that the S_{eq} is almost equal to the S_∞, which suggested that the swelling behaviors of the SPH in various pH solutions could reach equilibrium within 4 h, and the swelling process obeys Schott's swelling model. Furthermore, with altering the pH values of swelling medium, the S_{eq} and S_∞ values were initially increased with increasing the external pH to 6 and then keep almost constant in the pH range of 6–8. The further increase of pH from 10 to 12 causes a steep decrease of S_{eq} and S_∞. The pH-dependent swelling behavior is due to the ionization of carboxylic groups after the external pH values exceeding its pK_a (approximately 4.6), and thus the gel network tends to swell more. The shrinkage of the network in basic environment (pH > 10) is mainly attributed to the shielding effect of counter-ions (Na^+) with high mobility on negatively charged hydrophilic groups.

The change tendency of k_{is} as a function of pH values is similar with the S_{eq} and S_∞ (Fig. 6d). As described previously (Yin, Yang, & Xu, 2001), the initial swelling rate of the hydrogel is usually related to the relaxation rate of the chain segments in the network. The ionization of —COOH groups occurs at pH > 4.6 and this trend is increased at higher pH. The increased —COO^- groups led to a stronger electrostatic repulsion, which benefit to the relaxation of the polymer network. The fast relaxation is favorable to the penetration of water molecules into the gel network more easily, and so the initial swelling rate can be enhanced. However, the mobility of the polymer network is reduced by the shielding effect of cations when pH > 10, suggesting that the diffusion of water molecules into the polymer network was limited and the initial swelling rate was decreased.

4. Conclusions

A novel NaAlg-based SPH was prepared by grafting NaA and St onto NaAlg backbones in the presence of initiator APS and crosslinker MBA, using the self-assembled SDS micelle as a pore-forming template. FTIR spectra confirmed that the grafting

copolymerization reaction occurred and SDS was removed from the final product during washing process. The SDS concentration strongly affected the morphologies and pore structure as shown by SEM and BET results. The SDS concentration of 1.92 mM facilitates to form a homogeneous and well-defined pore structure, and the SPH corresponding to 1.92 mM SDS shows higher swelling ratio and swelling rate. The improvement of swelling is mainly due to the looser network structure and larger surface area. The salt, external pH has greater influence on the time-dependent swelling behaviors of the SDS-1.92 mM SPH, and the swelling of the hydrogel in multivalent salt (Ca^{2+}, Al^{3+})/pH 2 solutions exhibited a well-known "overshooting effect" resulting from the ionic-crosslinking and hydrogen-bonding interaction. The time-dependent swelling of the SPH in Na^+/pH 3–12 solutions followed Schott's second-order swelling kinetics model, and the increase of Na^+ concentration decreased the kinetic parameter (k_{is}). Additionally, the swelling rate constant increased when pH is lower than 8, but decreased when pH is greater than 10. This indicates the initial swelling of the SPH in pH $\leq$ 8 solutions depends on the diffusion rate of water molecules and the relaxation of polymer chains. However, in pH > 10 solutions, the swelling of the SPH is mainly controlled by the diffusion rate of water molecules into the polymeric network.

Acknowledgements

The authors gratefully acknowledge jointly supporting of this research by the National Natural Science Foundation of China (No. 20877077) and the Open Fund of the Key Laboratory of Chemistry of Northwestern Plant Resources, China Academy of Sciences (No. CNPR2010kfkt01).

References

Almeida, J. F., Ferreira, P., Lopes, A., & Gil, M. H. (2011). Photocrosslinkable biodegradable responsive hydrogels as drug delivery systems. *International Journal of Biological Macromolecules*, *49*, 948–954.

Augst, A. D., Kong, H. J., & Mooney, D. J. (2006). Alginate hydrogels as biomaterials. *Macromolecular Bioscience*, *6*, 623–633.

Barbetta, A., Barigelli, E., & Dentini, M. (2009). Porous alginate hydrogels: Synthetic methods for tailoring the porous texture. *Biomacromolecules*, *10*, 2328–2337.

Busby, W., Cameron, N. R., & Jahoda, C. A. B. (2001). Emulsion-derived foams (polyHIPEs) containing poly(epsilon-caprolactone) as matrixes for tissue engineering. *Biomacromolecules*, *2*, 154–164.

Cameron, N. R. (2005). High internal phase emulsion templating as a route to well-defined porous polymers. *Polymer*, *46*, 1439–1449.

Cha, C., Kim, E. S., Kim, I. W., & Kong, H. (2011). Integrative design of a poly(ethylene glycol)–poly(propylene glycol)-alginate hydrogel to control three dimensional biomineralization. *Biomaterials*, *32*, 2695–2703.

Chang, C. Y., Duan, B., Cai, J., & Zhang, L. N. (2010). Superabsorbent hydrogels based on cellulose for smart swelling and controlled delivery. *European Polymer Journal*, *46*, 92–100.

Chatterjee, S., Chatterjee, T., & Woo, S. H. (2010). A new type of chitosan hydrogel sorbent generated by anionic surfactant gelation. *Bioresource Technology*, *101*, 3853–3858.

Chatterjee, S., Lee, D. S., Lee, M. W., & Woo, S. H. (2010). Enhanced molar sorption ratio for naphthalene through the impregnation of surfactant into chitosan hydrogel beads. *Bioresource Technology*, *101*, 4315–4321.

Delaney, J. T., Liberski, A. R., Perelaer, J., & Schubert, U. S. (2010). Reactive inkjet printing of calcium alginate hydrogel porogens—A new strategy to open-pore structured matrices with controlled geometry. *Soft Matter*, *6*, 866–869.

Draget, K. I., SkjakBraek, G., & Smidsrod, O. (1997). Alginate based new materials. *International Journal of Biological Macromolecules*, *21*, 47–55.

Dumitriu, R. P., Mitchell, G. R., & Vasile, C. (2011). Rheological and thermal behaviour of poly(N-isopropylacrylamide)/alginagte smart polymeric networks. *Polymer International*, *60*, 1398–1407.

Elbert, D. L. (2011). Liquid–liquid two-phase systems for the production of porous hydrogels and hydrogel microspheres for biomedical applications: A tutorial review. *Acta Biomaterialia*, *7*, 31–56.

Foungfung, D., Phattanarudee, S., Seetapan, N., & Kiatkamjornwong, S. (2011). Acrylamide-itaconic acid superabsorbent polymers and superabsorbent polymer/mica nanocomposites. *Polymers advanced Technologies*, *22*, 635–647.

Gils, P. S., Ray, D., & Sahoo, P. K. (2009). Characteristics of xanthan gum-based biodegradable superporous hydrogel. *International Journal of Biological Macromolecules*, *45*, 364–371.

Jia, K., Young, Y. K., & Moo, H. K. (2011). Polysaccharide-based superporous hydrogels with fast swelling and superabsorbent properties. *Carbohydrate Polymers*, *83*, 284–290.

Ji, C. D., Khademhosseini, A., & Dehghani, F. (2011). Enhancing cell penetration and proliferation in chitosan hydrogels for tissue engineering applications. *Biomaterials*, *32*, 9719–9729.

Kabiri, K., Lashani, S., Zohuriaan-Mehr, M. J., & Kheirabadi, M. (2011). Super alcohol-absorbent gels of sulfonic acid-contained poly(acrylic acid). *Journal of Polymer Research*, *18*, 449–458.

Krušić, M. K., & Filipovic, J. (2006). Copolymer hydrogels based on *N*-isopropylacrylamide and itaconic acid. *Polymer*, *47*, 148–155.

Lee, E. A., Balakrishnan, P., Song, C. K., Choi, J. H., Noh, G. Y., Park, C. G., et al. (2010). Microemulsion-based hydrogel formulation of itraconazole for topical delivery. *Journal of Pharmaceutical Investigation*, *40*, 305–311.

Marsano, E., Bianchi, E., & Sciutto, L. (2003). Microporous thermally sensitive ethyleneglicol diglycidyl ether. *Polymer*, *44*, 6835–6843.

Ozay, O., Ekici, S., Baran, Y., Aktas, N., & Sahiner, N. (2009). Removal of toxic metal ion with magnetic hydrogels. *Water Research*, *43*, 4403–4411.

Pang, S. C., Chin, S. F., Tay, S. H., & Tchong, F. M. (2011). Starch-maleate-polyvinyl alcohol hydrogels with controllable swelling behaviors. *Carbohydrate Polymers*, *84*, 424–429.

Park, H., & Kim, D. (2006). Swelling and mechanical properties of glycol chitosan/poly(vinyl alcohol) IPN-type superporous hydrogels. *Journal of Biomedical Materials Research Part A*, *78A*, 662–667.

Partap, S., Muthutantri, A., Rehman, I. U., Davis, G. R., & Darr, J. A. (2007). Preparation and characterization of controlled porosity alginate hydrogels made via a simultaneous micelle templating and internal gelation process. *Journal of Material Science*, *42*, 3502–3507.

Partap, S., Rehman, I., Jones, J. R., & Darr, J. A. (2006). Supercritical carbon dioxide in water emulsion-templated synthesis of porous calcium alginate hydrogels. *Advanced Materials*, *18*, 501–504.

Pourjavadi, A., Hosseinzadeh, H., & Sadeghi, M. (2007). Synthesis, characterization and swelling behavior of gelatin-*g*-poly(sodium acrylate)/kaolin superabsorbent hydrogel composites. *Journal of Composite Materials*, *41*, 2057–2069.

Poursamara, S. A., Azamib, M., & Mozafari, M. (2011). Controllable synthesis and characterization of porous polyvinyl alcohol/hydroxyapatite nanocomposite scaffolds via an in situ colloidal technique. *Colloids and Surfaces B: Biointerfaces*, *84*, 310–316.

Rosa, F., Bordado, J., & Casquilho, M. (2002). Kinetics of water absorbency in AA/AMPS copolymers: Applications of a diffusion-relaxation model. *Polymer*, *43*, 63–70.

Sand, A., Yadav, M., Mishra, D. K., & Behari, K. (2010). Modification of alginate by grafting of N-vinyl-2-pyrrolidone and studies of physicochemical properties in terms of swelling capacity, metal-ion uptake and flocculation. *Carbohydrate Polymers*, *80*, 1147–1154.

Schott, H. (1992). Swelling kinetics of polymers. *Journal of Macromolecular Science Part B: Physics*, *31*, 1–9.

Shi, X. N., Wang, W. B., & Wang, A. Q. (2011a). Synthesis and enhanced swelling properties of a guar gum-based superabsorbent composite by the simultaneous introduction of styrene and attapulgite. *Journal of Polymer Research*, *18*, 1705–1713.

Shi, X. N., Wang, W. B., & Wang, A. Q. (2011b). Effect of surfactant on porosity and swelling behaviors of guar gum-*g*-poly(sodium acrylate-co-styrene)/attapulgite superabsorbent hydrogels. *Colloids and Surfaces B: Biointerfaces*, *88*, 279–286.

Shi, X. N., Wang, W. B., Kang, Y. R., & Wang, A. Q. (2012). Enhanced swelling properties of a novel sodium alginate-based superabsorbent composites: NaAlg-*g*-poly(NaA-*co*-St)/APT. *Journal of Applied Polymer Science*, *125*, 1822–1832.

Su, J. C., Liu, S. Q., Joshi, S. C., & Lam, Y. C. (2008). Effect of SDS on the gelation of hydroxypropylmethylcellulose hydrogels. *Journal of Thermal Analysis and Calorimetry*, *93*, 495–501.

Van Vlierberghe, S., Dubruel, P., & Schacht, E. (2011). Biopolymer-based hydrogels as scaffolds for tissue engineering applications: A review. *Biomacromolecules*, *12*, 1387–1408.

Wang, W. B., & Wang, A. Q. (2010). Nanocomposite of carboxymethyl cellulose and attapulgite as a novel pH-sensitive superabsorbent: Synthesis, characterization and properties. *Carbohydrate Polymers*, *82*, 83–91.

Yang, L. L., Ma, X. Y., & Guo, N. N. (2011). Synthesis and properties of sodium alginate/Ne(+) rectorite grafted acrylic acid composite superabsorbent via (60)Co gamma irradiation. *Carbohydrate Polymers*, *85*, 413–418.

Yin, L. C., Ding, J. Y., Zhang, J., He, C. B., Tang, C., & Yin, C. H. (2010). Polymer integrity related absorption mechanism of superporous hydrogel containing interpenetrating polymer networks for oral delivery of insulin. *Biomaterials*, *31*, 3347–3356.

Yin, Y. H., Yang, Y. J., & Xu, H. B. (2001). Hydrogels for colon-specific drug delivery: Swelling kinetics and mechanism of degradation in vitro. *Journal of Polymer Science Part B: Physics*, *39*, 3128–3137.

Zhao, Y., Su, H. J., Fang, L., & Tan, T. W. (2005). Superabsobent hydrogels from poly(aspartic acid) with salt-, temperature- and pH-responsiveness properties. *Polymer*, *46*, 5368–5376.

Zhou, Y. S., Ma, G. P., Shi, S. Q., Yang, D. Z., & Nie, J. (2011). Photopolymerized water-soluble chitosan-based hydrogel as potential use in tissue engineering. *International Journal of Biological Macromolecules*, *48*, 408–413.

Zohuriaan-Mehr, M. J., Omidian, H., Doroudiani, S., & Kabiri, K. (2010). Advances in non-hygienic applications of superabsorbent hydrogel materials. *Journal of Materials Science*, *45*, 5711–5735.